Noname manuscript No.
(will be inserted by the editor)

Modeling final-state interactions with a relativistic multiple-scattering approximation

"Relativistic Description of Two- and Three-Body Systems in Nuclear Physics", ECT*, October 19-13 2009

W. Cosyn · J. Ryckebusch

Received: date / Accepted: date

Abstract We address the issue of nuclear attenuation in nucleon and pion knockout reactions. A selection of results from a model based on a relativistic multiple-scattering approximation is presented. We show transparency calculations for pion electroproduction on several nuclei, where data are in very good agreement with calculations including color transparency. Secondly, we discuss the density dependence of reactions involving one or double proton knockout. The latter reaction succeeds in probing the high density regions in the deep interior of the nucleus.

Keywords Relativistic scattering theory

PACS 25.30.Rw,25.40.Ep,24.10.Jv,24.10.-i,11.80.-m,11.80.La

1 Introduction

It is an open issue how and at what energy scale hadrons emerge from quarks and gluons, the fundamental constituents of quantum chromodynamics. The behavior of nucleons in a nucleus is another topic of great interest and this can be studied by exploring the limits of the shell-model description of nuclei. This can be achieved, for instance, by looking at the medium modifications of hadron properties, the density dependence of the nucleon-nucleon interactions, or the properties of the nucleon-nucleon correlations at very short internucleon distances.

These fascinating issues can be experimentally explored at facilities that can probe the nucleonic and sub-nucleonic length scales, such as Jefferson lab, J-PARC, and FAIR. Various aspects of nuclear structure can be studied in reactions such as $A(e,e'p)$, $A(e,e'\pi)$, $A(p,2p)$, $A(\gamma,2p)$, etc., whereby a fast leptonic or hadronic probe ejects one or more hadrons from the target nucleus. To interpret the data from these experiments, one needs models that can quantify the effect of nuclear attenuation on the impinging and ejected nucleons and pions. These model calculations can for example be used to identify QCD-mediated deviations from traditional nuclear physics predictions and to map the density regions of nuclei contributing to the cross section of some specific reaction.

Here, we present a selection of results obtained in a model based on a relativistic extension of Glauber multiple-scattering theory for the description of nuclear attenuation on the impinging hadrons (initial-state interactions, ISI) or ejected hadrons (final-state interactions, FSI). This relativistic multiple-scatttering Glauber approximation (RMSGA) model provides a comprehensive theoretical framework that can be used for a variety of leptonic and hadronic probes and one or more outgoing nucleons and/or pions. The RMSGA model has no free parameters. It is used to calculate several observables like cross sections and nuclear transparencies. The general features of the model are introduced in Sec. 2 and some results are shown in Sec. 3.

W. Cosyn
Department of Physics and Astronomy,
Ghent University, Proeftuinstraat 86, B-9000 Gent, Belgium
E-mail: wim.cosyn@ugent.be
Present address: Florida International University, Miami, Florida 33199, USA

J. Ryckebusch
Department of Physics and Astronomy,
Ghent University, Proeftuinstraat 86, B-9000 Gent, Belgium

2 Relativistic multiple-scattering Glauber approximation

Glauber multiple-scattering theory can be applied when the wavelength of the scattering particle is small in comparison with the typical interaction range between the scatterer and the spectator particles. Examples of such kinematic conditions will be discussed in Sec. 3, with nucleon and pion energies in the range of a few GeV. Originating from optics, Glauber theory uses the eikonal approximation for high energy particles scattering under small angles. A relativistic extension of this eikonal approximations was developed and has been applied to $A(e,e'p)$ reactions [1,2], $A(p,2p)$ processes [3,4], pion photo- and electroproduction reactions [5,6] and neutrino-induced nucleon knockout [7]. Relativity is accommodated both in the kinematics and dynamics, and all hadrons involved in the reaction process are described by relativistic wave functions. The impulse approximation is used for the interaction of the beam particle with the target.

As an example we mention the Glauber phase in the RMSGA model entering the amplitude for a reaction with an impinging proton which has i hadrons in the final state

$$\mathcal{G}(\mathbf{b},z) = \prod_{\alpha_{occ}\neq\alpha} \int d\mathbf{r}' \left|\phi_{\alpha_{occ}}(\mathbf{r}')\right|^2 \times \left[1-\theta\left(z-z'\right)\Gamma_{pN}\left(\mathbf{b}'-\mathbf{b}\right)\right] \times \prod_i \left[1-\theta\left(z_i'-z_i\right)\Gamma_{iN}\left(\mathbf{b}_i'-\mathbf{b}_i\right)\right]. \quad (1)$$

Here, α stands for the quantum numbers of the nucleon that interacts with the initial probe, $\mathbf{r}=(\mathbf{b},z)$ is the coordinate of the hard interaction, with z along the momentum of the impinging hadron. The coordinate $\mathbf{r}_i=(\mathbf{b}_i,z_i)$ is defined such that the z_i axis is along the direction of the momentum of the ejected hadron i. The $\mathbf{r}_i'=(\mathbf{b}_i',z_i')$ denotes the coordinate $\mathbf{r}'$ in the reference system defined by $\mathbf{r}_i$.

The product α_{occ} runs over all residual nucleons, with $\phi_{\alpha_{occ}}(\mathbf{r}')$ the single particle bound-state wave functions obtained from the Serot-Walecka model [8]. The Heaviside function ensures that only nucleons in the backward path of the impinging hadron and nucleons in the forward path of the ejected hadrons can make contributions to their phase. Information on the ISI and FSI is contained in the profile function, and the product i runs over all particles subject to nuclear attenuations. The profile function Γ_{iN} for nucleon-nucleon and pion-nucleon scattering depends on three energy-dependent parameters and has a Gaussian form:

$$\Gamma_{iN}(\mathbf{b}) = \frac{\sigma_{iN}^{\rm tot}(1-i\epsilon_{iN})}{4\pi\beta_{iN}^2}\exp\left(-\frac{\mathbf{b}^2}{2\beta_{iN}^2}\right) \text{ (with } i=\pi \text{ or } N'). \quad (2)$$

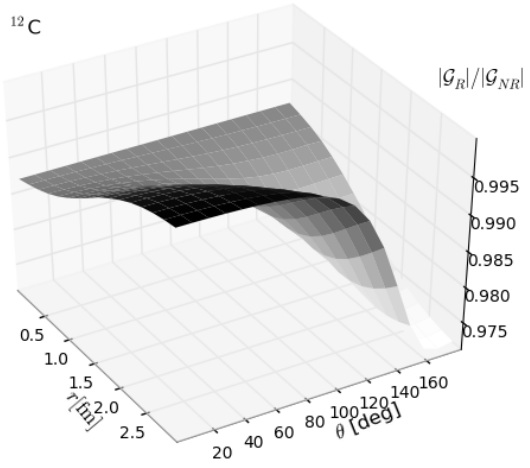

Fig. 1: The effect of the lower components in the wave functions for the scattering centers on the computed Glauber phase $\mathcal{G}$ at $p=1.5$ GeV for proton emission from ^{12}C. The figure shows the ratio of the norm of the Glauber phase as computed with the full relativistic single-particle wave function to the one which only retains the upper Dirac components. The $\mathcal{G}(\mathbf{b},z)$ is computed for a proton escaping along the z axis. The coordinates (r,θ) indicate the position of the initial absorption process which triggers the reaction.

The three parameters $\sigma_{iN}^{\rm tot},\epsilon_{iN},\beta_{iN}$, are fitted to nucleon-nucleon and pion-nucleon scattering data [9,10,11].

The scalar Glauber phase $\mathcal{G}(\mathbf{b},z)$ is a complex quantity which encodes the combined effect of attenuation for a specific exclusive reaction that is initiated at the position $\mathbf{r}(\mathbf{b},z)$. The deviation of the norm $|\,\mathcal{G}(\mathbf{b},z)\,|$ from 1 is a measure of the magnitude of nuclear attenuation.

In our relativistic formulation of Glauber multiple-scattering theory the single-particle densities $\left|\phi_{\alpha_{occ}}(\mathbf{r}')\right|^2$ in Eq. (1) contain an upper and lower component. It is conjectured that the effect of relativity on the magnitude of the nuclear attenuation can be estimated by the relative contribution from the lower components. Fig. 1 shows the effect of the lower components of the single particle densities on the Glauber phase of an outgoing particle with an energy representative for the few GeV range. This shows that the effect of relativity on the computed magnitude of nuclear attenuation is rather small, typically a few percent.

It can be expected that the nucleon-nucleon and pion-nucleon profile functions entering Eq. (1) will be subject to medium modifications [12]. Mechanisms like Pauli blocking often lead to an effective reduction of the nucleon-nucleon cross sections in the medium. At higher energies the effect of Pauli blocking is small. Another impor-

tant source of medium effects are short-range correlations. Short-range correlations (SRC) can be included in the treatment of the Glauber eikonal phase by using the information that a nucleon is present at the coordinate of the hard interaction.

This can be achieved in the following way. First, the squared single-particle wave functions in Eq. (1) can be approximated by the one-body density of the target nucleus $\rho_A^{[1]}(\mathbf{r})$ defined as

$$|\phi_\alpha(\mathbf{r})|^2 \to \frac{\rho_A^{[1]}(\mathbf{r})}{A} = \int d\mathbf{r}_2 \ldots \int d\mathbf{r}_A \left(\Psi_A^{\text{g.s.}}(\mathbf{r},\mathbf{r}_2,\ldots,\mathbf{r}_A)\right)^\dagger \times \Psi_A^{\text{g.s.}}(\mathbf{r},\mathbf{r}_2,\ldots,\mathbf{r}_A).$$

Here, $\Psi_A^{\text{g.s.}}$ is the ground-state wave function of the target nucleus, obtained by antisymmetrizing the product of the single-particle wave functions ϕ_α. This substitution has minor effects on the results obtained in the RMSGA model [1]. In a next step , the averaged density $\rho_A^{[1]}(\mathbf{r})$ can be substituted with the ratio of the two-body density $\rho_A^{[2]}$ (normalized as $\int d\mathbf{r}_1 \int d\mathbf{r}_2 \rho_A^{[2]}(\mathbf{r}_1,\mathbf{r}_2) = A(A-1)$) and the one-body density:

$$\rho_A^{[1]}(\mathbf{r}_2) \to \frac{A}{A-1}\frac{\rho_A^{[2]}(\mathbf{r}_2,\mathbf{r})}{\rho_A^{[1]}(\mathbf{r})}, \tag{3}$$

where $\mathbf{r}$ is the coordinate of the hard interaction. In the case of an uncorrelated two-body density:

$$\rho_{A,\text{uncorr.}}^{[2]}(\mathbf{r}_1,\mathbf{r}_2) \equiv \frac{A-1}{A}\rho_A^{[1]}(\mathbf{r}_1)\rho_A^{[1]}(\mathbf{r}_2), \tag{4}$$

and Eq. (3) becomes trivial. One can include SRC in the two-body density by adopting the following functional form [13]:

$$\rho_{A,\text{corr.}}^{[2]}(\mathbf{r}_1,\mathbf{r}_2) \equiv \frac{A-1}{A}\gamma(\mathbf{r}_1)\rho_A^{[1]}(\mathbf{r}_1)\rho_A^{[1]}(\mathbf{r}_2)\gamma(\mathbf{r}_2)g(r_{12}), \tag{5}$$

where $g(r_{12})$ is the so-called Jastrow correlation function and $\gamma(\mathbf{r})$ a function that imposes the normalization of the two-body density obtained as the solution of an integral equation. With the above expression for the two-body density , Eq. (3) becomes

$$\rho_A^{[1]}(\mathbf{r}_2) \to \gamma(\mathbf{r}_2)\rho_A^{[1]}(\mathbf{r}_2)\gamma(\mathbf{r})g(|\mathbf{r}_2-\mathbf{r}|) \equiv \rho_A^{\text{eff}}(\mathbf{r}_2,\mathbf{r}). \tag{6}$$

With above derivation it is clear that the calculation of the FSI effects can be corrected for SRC by replacing $\left|\phi_{\alpha_{occ}}(\mathbf{r}')\right|^2$ with $\rho_A^{\text{eff}}(\mathbf{r}',\mathbf{r})/A$ in Eq. (1)

Colour transparency is a QCD mediated phenomenon that predicts reduced hadron-nucleon interactions that become more pronounced as the initial hadron production process occurs at smaller and smaller scales. The effect of colour transparency can be included in the RMSGA calculations by making use of the quantum diffusion model of Ref. [14] and replacing the total cross section parameter in Eq. (2) with an effective one that evolves from a reduced to its normal value along a certain formation length l_h:

$$\frac{\sigma_{iN}^{\text{eff}}(\mathscr{Z})}{\sigma_{iN}^{\text{tot}}} = \left\{\left[\frac{\mathscr{Z}}{l_h} + \frac{<n^2k_t^2>}{\mathscr{H}}\left(1-\left(\frac{\mathscr{Z}}{l_h}\right)\right)\right] \times \theta(l_h-\mathscr{Z}) + \theta(\mathscr{Z}-l_h)\right\}. \tag{7}$$

Here, n is the number of elementary fields (2 for the pion, 3 for the nucleon), $k_t = 0.350$ GeV/c is the average transverse momentum of a quark inside a hadron, and $\mathscr{H}$ is the hard-scale parameter (or virtuality) that governs the CT effect. For the formation length $l_h \approx 2p/\Delta M^2$, we adopt the values $\Delta M^2 = 1$ GeV^2 for the proton and $\Delta M^2 = 0.7$ GeV^2 for the pion.

3 Results

Transparencies First we show some results for transparency calculations in the RMSGA model. The transparency observable is used in the search for the emergence of partonic degrees of freedom in nuclear reactions and is defined as the ratio of the cross section on a nucleus to A times the cross section on a free proton. Figure 2 presents the results from our transparency calculations for the pion electroproduction ($A(e,e'\pi^+)$) reaction on four different nuclei, together with the experimental data [16] and results from the semiclassical model of Ref. [15]. The RMSGA and semiclassical transparencies display a modest increase over the Q^2 range. This behaviour finds a simple explanation in the p_π dependence of the $\sigma_{\pi^+p}^{\text{tot}}$. The results contained in Fig. 2 cover a range in pion momenta given by $2.8 \le p_\pi \le 4.4$ GeV. In this range, $\sigma_{\pi^+p}^{\text{tot}}$ displays a soft decrease, which reflects itself in a soft increase of the nuclear transparency. After including the effect of SRC (calculations referred to as RMSGA+SRC), the transparencies are about 2% larger for ^{12}C, ^{27}Al and ^{63}Cu, and about 4% larger for ^{197}Au. This reflects the fact that the medium effectively reduces the free pion-nucleon cross sections. It is obvious that the effect of SRC does not depend on the hard-scale parameter Q^2. The CT mechanism, on the other hand, shows a strong Q^2 dependence with CT-related enhancements up to 20% at the highest energies. These calculations including CT are in very good agreement with the experimental data. The results overestimate the Au data somewhat, but the slope is in agreement with the

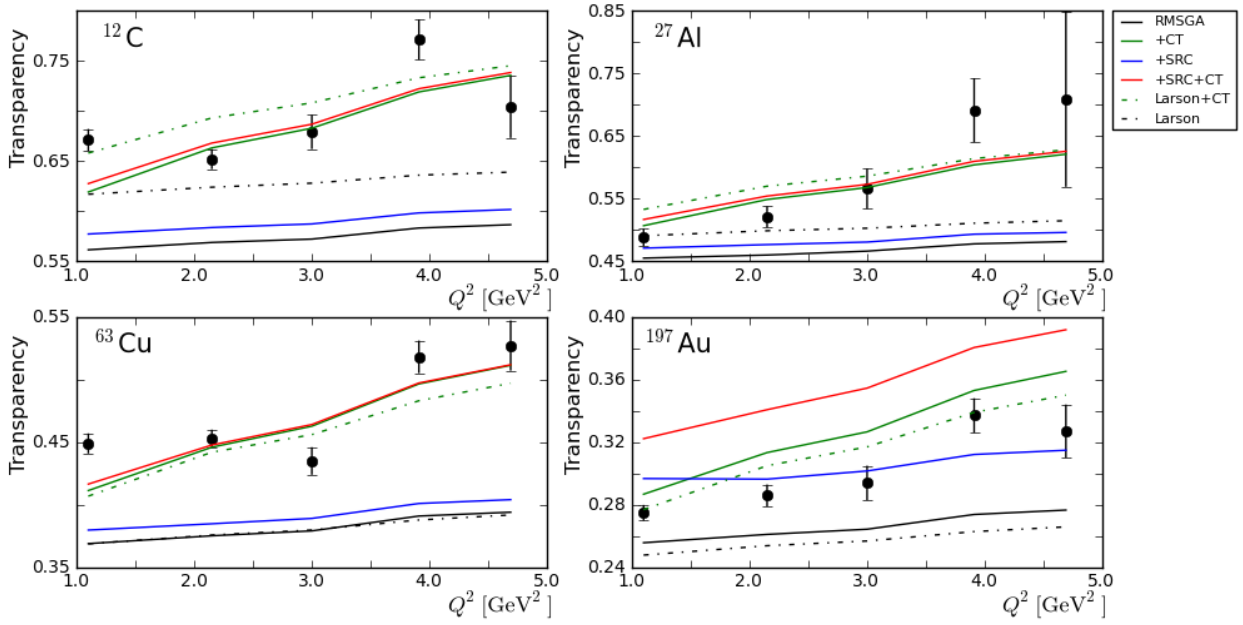

Fig. 2: *[Colour online]* The Q^2 dependence of the nuclear transparency for the $A(e,e'\pi^+)$ process in ^{12}C, ^{27}Al, ^{63}Cu and ^{197}Au. The dot-dashed curves are the results of the semi-classical model by Larson, Miller and Strikman [15]. JLab data are taken from Ref. [16].

data. Upon comparing the RMSGA+CT results to the semi-classical calculations, we see that the slopes of both calculations are in excellent agreement, reflecting the use of the same quantum diffusion parametrization for the CT effect. There are some differences in the predicted values of the transparencies between the semiclassical and the RMSGA model. The RMSGA predictions are somewhat larger for the ^{12}C target, and evolve to smaller for the ^{197}Au target. A more recent model developed by Kaskulov et al. [17] also finds excellent agreement between the calculations including CT and the data.

Density dependence We can also apply the RMSGA model to map which density regions of the target nucleus are effectively probed in a certain nucleon-knockout reaction [18]. The scattering parameters entering in the Glauber profile function of Eq. (2) show little energy dependence for nucleon or pion momenta above 1 GeV. This is reflected, for instance, in the soft energy dependence of the regular RMSGA transparencies in Fig. 2. The stronger Q^2 dependence observed in the data can be explained by the CT phenomenon. Together with the ability to deploy the RMSGA framework in a variety of reactions, this allows us to make statements about the role of nuclear attenuations on the effectively probed densities for a broad energy range.

For single-nucleon knockout reactions, we can study the density dependence of the reaction in a factorized approach by calculating $\delta(r,\theta)$, which represents the contribution to the distorted momentum distribution around r and θ and is defined as follows:

$$\begin{aligned}\rho^D_{n\kappa}(\mathbf{p}_m) &= \sum_{s,m}\left|\int d\mathbf{r}\frac{e^{-i\mathbf{p}_m\cdot\mathbf{r}}}{(2\pi)^3}\bar{u}(\mathbf{p}_m,s)\mathcal{G}^\dagger(\mathbf{r})\phi_{n\kappa m}(\mathbf{r})\right|^2 ,\\ &= \iint dr d\theta\frac{1}{2}\left[\sum_{s,m}\left((D(r,\theta))^\dagger\iint dr'd\theta' D(r',\theta')\right.\right.\\ &\quad \left.\left.+D(r,\theta)\iint dr'd\theta'\left(D(r',\theta')\right)^\dagger\right)\right] ,\\ &\equiv \iint dr d\theta\delta(r,\theta) \ . \end{aligned} \tag{8}$$

In this equation, $\phi_{n\kappa m}(\mathbf{r})$ is the single-particle wave function of the struck nucleon (with quantum numbers $(n\kappa m)$), the missing momentum $\mathbf{p}_m = \mathbf{q}-\mathbf{p}$ is defined as the difference between the momentum transfer and the final nucleon momentum, and the function $D(r,\theta)$ is defined as

$$D(r,\theta) = \int d\phi\, r^2\sin\theta\frac{e^{-i\mathbf{p}_m\cdot\mathbf{r}}}{(2\pi)^3}\bar{u}(\mathbf{p}_m,s)\mathcal{G}^\dagger(\mathbf{r})\phi_{n\kappa m}(\mathbf{r}) . \tag{9}$$

In the factorized approach, the cross section is proportional to the distorted momentum distribution $\rho^D_{n\kappa}(\mathbf{p}_m)$, and $\delta(r,\theta)$ thus provides a measure for the contributions to the cross section of the different density regions in the nucleus.

Results for $\delta(r,\theta)$ for the ^{12}C$(e,e'p)$ and ^{12}C$(p,2p)$ reactions are shown in Fig. 3 with θ measured from the

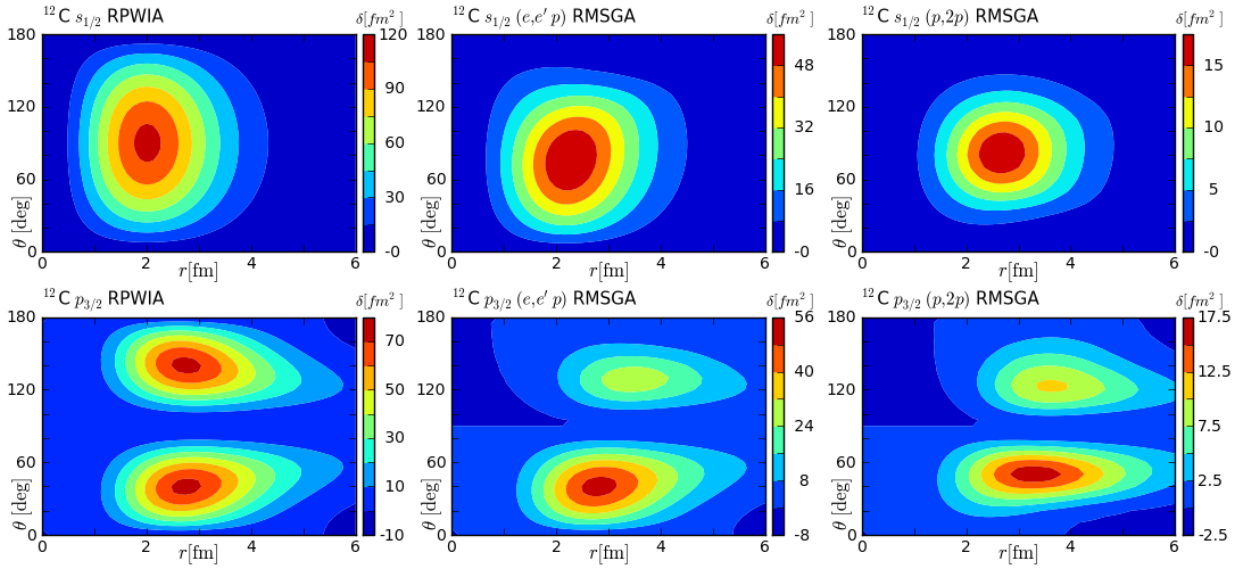

Fig. 3: *[Colour online]* The function $\delta(r,\theta)$ for the ^{12}C$(e,e'p)$ and ^{12}C$(p,2p)$ reactions. The energy transfer for both reactions is 1.5 GeV and the three-momentum transfer $\mathbf{q}$ is tuned to probe the maximum of the momentum distribution (i.e. p_m=0 MeV for knockout from the $s1/2$-orbit and p_m=115 MeV for removal from the $p3/2$-orbit). The proton is ejected along $\mathbf{q}$ for the $(e,e'p)$ results. For the $(p,2p)$ calculations, both protons in the final state have 1.5 GeV kinetic energy and are detected under an angle of 32° on opposite sides of the incoming proton. This particular kinematic situation is often referred to as coplanar and symmetric kinematics. For the sake of reference, the proton root-mean-square radius in ^{12}C as determined from elastic electron scattering is $\left\langle r^2\right\rangle^{1/2} = 2.464 \pm 0.012$ fm [19].

direction of momentum transfer and r denoting the distance relative to the center of the target nucleus. The energy transfer is 1.5 GeV and the polar angle of the ejected protons are determined such that the kinematics probes the maximum of the undisturbed momentum distribution. In the relativistic plain-wave (RPWIA) limit, no ISI or FSI are present ($\mathcal{G}(\mathbf{r}) \equiv 1$) and $\delta(r,\theta)$ is equal for $(e,e'p)$ and $(p,2p)$. For the selected kinematics described in the caption to Fig. 3, there is a symmetry-axis for $\theta = 90°$. In the absence of any effect stemming from nuclear attenuation the forward and backward hemispheres equally contribute. After including the FSI and/or ISI in the RMSGA approach, we observe that the nuclear attenuations reduce the value of $\delta(r,\theta)$, shift the maximum values to higher values of r, and also induce an asymmetry in the θ direction. The biggest contributions to the cross section stem from the forward hemisphere. The relative contribution from the interior regions of large target-nucleus density gets reduced due to its sensitivity to strong FSI mechanisms. All these effects are more pronounced in the $(p,2p)$ reaction, where three (one incoming, two outgoing) protons are subject to the attenuations and the biggest contributions are close to the nuclear surface.

To formulate the equivalent of Eq. (8) for two-nucleon knockout reactions such as $A(\gamma,pp)$ in a factorized approach, we have to assume that the proton pair resides in a relative S-state. This is a reasonable approximation as investigations of the ^{16}O$(e,e'pp)$ reaction at the electron accelerators in Mainz [20,21] and Amsterdam [22, 23,24] have clearly shown that pairs of protons are solely subject to short-range correlations when they reside in a relative S state under conditions corresponding with relatively small c.m. momenta P (or, the initial protons are very close and moving back-to-back). This assumption allows us to write a distorted momentum distribution for the nucleon-nucleon pair:

$$\rho^D_{n_1\kappa_1,n_2\kappa_2}(\mathbf{P}) = \sum_{s_1,s_2,m_1,m_2} \left| \int d\mathbf{R} \frac{e^{-i\mathbf{P}_m\cdot\mathbf{R}}}{(2\pi)^3} \bar{u}(\mathbf{p}+\frac{\mathbf{P}}{2},s_1) \times \phi_{n_1\kappa_1 m_1}(\mathbf{R}) \bar{u}(-\mathbf{p}+\frac{\mathbf{P}}{2},s_2) \phi_{n_2\kappa_2 m_2}(\mathbf{R}) \mathcal{G}^\dagger(\mathbf{R}) \right|^2 \equiv \iint dR d\theta \delta(R,\theta) \ , \quad (10)$$

with $\mathbf{P}$ ($\mathbf{p}$) the center of mass momentum (relative momentum) of the outgoing nucleon-nucleon pair. The missing momentum $\mathbf{P}_m = \mathbf{P} - \mathbf{q}$ can be interpreted in the quasi-free approximation as the center of mass momentum of the correlated pair before the photon interaction.

Fig. 4 shows $\delta(R,\theta)$ for the dual proton knockout on ^{12}C, with proton kinetic energies of 1.5 GeV in the final

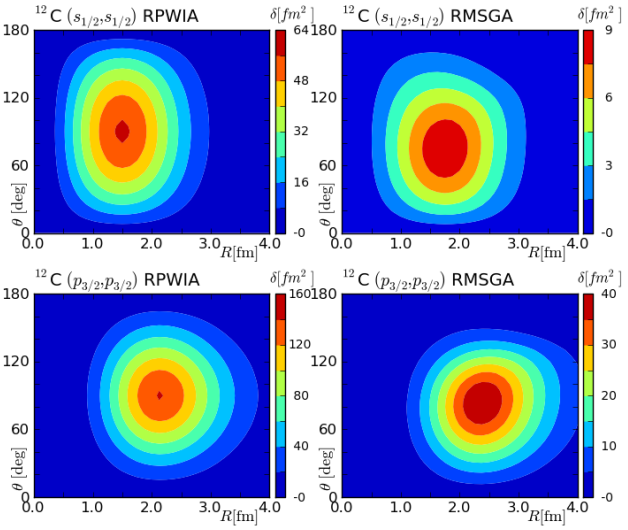

Fig. 4: *[Colour online]* The function $\delta(R,\theta)$ for the exclusive ^{12}C(γ,pp) cross section. We consider an energy transfer of 3 GeV and a three-momentum transfer **q** that is tuned to probe the maximum of the momentum distribution $\rho_{n_1\kappa_1,n_2\kappa_2}(\mathbf{P})$ (i.e. P=0 MeV for knockout from the $(s1/2-s1/2)$- and $(p3/2-p3/2)$-orbits). We consider coplanar and symmetric kinematics, i.e. the two escaping protons have the same energy and polar angle θ_{pq}, but escape from the opposite side of **q**

state. We can again quantity the effect of FSI by comparing the RMSGA to the RPWIA results. It is clear that the biggest values of $\delta(R,\theta)$ are situated much closer to the center than for the one-nucleon knockout reactions. Consequently, the $A(\gamma,pp)$ reaction succeeds in probing the high density regions of the target nucleus.

4 Conclusion

We have shown a selection of results obtained in a model based on relativistic multiple-scattering Glauber scattering theory. The model has no free parameters and can be applied to variety of reactions, with leptonic and hadronic beams and outgoing nucleons and/or pions. Our calculations show that relativity plays a rather modest role in the magnitude of nuclear attenuation. We showed very good agreement of pion transparencies with calculations including colour transparency. Secondly, we exploited the robustness of the model to explore which target-nucleus densities can be effectively probed in knockout reactions involving one, two and three protons. We find that the $A(\gamma,pp)$ reaction probes the interior of the target nucleus, the $A(p,2p)$ is rather peripheral, whereas the $A(e,e'p)$ is somewhat intermediate between these two.

Acknowledgements This work was supported by the Research Foundation Flanders and the Research Board of Ghent University.

References

1. J. Ryckebusch, et al., Nucl. Phys. **A728**, 226 (2003). DOI 10.1016/j.nuclphysa.2003.08.022
2. P. Lava, M.C. Martinez, J. Ryckebusch, J.A. Caballero, J.M. Udias, Phys. Lett. **B595**, 177 (2004). DOI 10.1016/j.physletb.2004.04.088
3. B. Van Overmeire, W. Cosyn, P. Lava, J. Ryckebusch, Phys. Rev. **C73**, 064603 (2006). DOI 10.1103/PhysRevC.73.064603
4. B. Van Overmeire, J. Ryckebusch, Phys. Lett. **B644**, 304 (2007). DOI 10.1016/j.physletb.2006.11.060
5. W. Cosyn, M.C. Martinez, J. Ryckebusch, B. Van Overmeire, Phys. Rev. **C74**, 062201 (2006). DOI 10.1103/PhysRevC.74.062201
6. W. Cosyn, M.C. Martinez, J. Ryckebusch, Phys. Rev. **C77**, 034602 (2008). DOI 10.1103/PhysRevC.77.034602
7. M.C. Martinez, et al., Phys. Rev. **C73**, 024607 (2006). DOI 10.1103/PhysRevC.73.024607
8. R.J. Furnstahl, B.D. Serot, H.B. Tang, Nucl. Phys. **A615**, 441 (1997). DOI 10.1016/S0375-9474(96)00472-1
9. W.M. Yao, et al., J. Phys. **G33**, 1 (2006). DOI 10.1088/0954-3899/33/1/001
10. T. Lasinski, R. Levi Setti, B. Schwarzschild, P. Ukleja, Nucl. Phys. **B37**, 1 (1972). DOI 10.1016/0550-3213(71)90316-6
11. R.A. Arndt, W.J. Briscoe, I.I. Strakovsky, R.L. Workman, M.M. Pavan, Phys. Rev. **C69**, 035213 (2004). DOI 10.1103/PhysRevC.69.035213
12. C.A. Bertulani, C. De Conti, Phys. Rev. **C81**, 064603 (2010). DOI 10.1103/PhysRevC.81.064603
13. S. Frankel, W. Frati, N. Walet, Nucl. Phys. **A580**, 595 (1994). DOI 10.1016/0375-9474(94)90783-8
14. L.L. Frankfurt, M.I. Strikman, Phys. Rept. **160**, 235 (1988). DOI 10.1016/0370-1573(88)90179-2
15. A. Larson, G.A. Miller, M. Strikman, Phys. Rev. **C74**, 018201 (2006). DOI 10.1103/PhysRevC.74.018201
16. B. Clasie, et al., Phys. Rev. Lett. **99**, 242502 (2007). DOI 10.1103/PhysRevLett.99.242502
17. M.M. Kaskulov, K. Gallmeister, U. Mosel, Phys. Rev. **C79**, 015207 (2009). DOI 10.1103/PhysRevC.79.015207
18. W. Cosyn, J. Ryckebusch, Phys. Rev. **C80**, 011602 (2009). DOI 10.1103/PhysRevC.80.011602
19. W. Reuter, G. Fricke, K. Merle, H. Miska, Phys. Rev. **C26**, 806 (1982). DOI 10.1103/PhysRevC.26.806
20. J. Ryckebusch, W. Van Nespen, Eur. Phys. J. **A20**, 435 (2004). DOI 10.1140/epja/i2003-10167-2
21. G. Rosner, Progress in Particle and Nuclear Physics **44**, 99 (2000). DOI DOI:10.1016/S0146-6410(00)00063-6
22. C.J.G. Onderwater, et al., Phys. Rev. Lett. **78**, 4893 (1997). DOI 10.1103/PhysRevLett.78.4893
23. C.J.G. Onderwater, et al., Phys. Rev. Lett. **81**, 2213 (1998). DOI 10.1103/PhysRevLett.81.2213
24. R. Starink, et al., Phys. Lett. **B474**, 33 (2000). DOI :10.1016/S0370-2693(99)01510-5